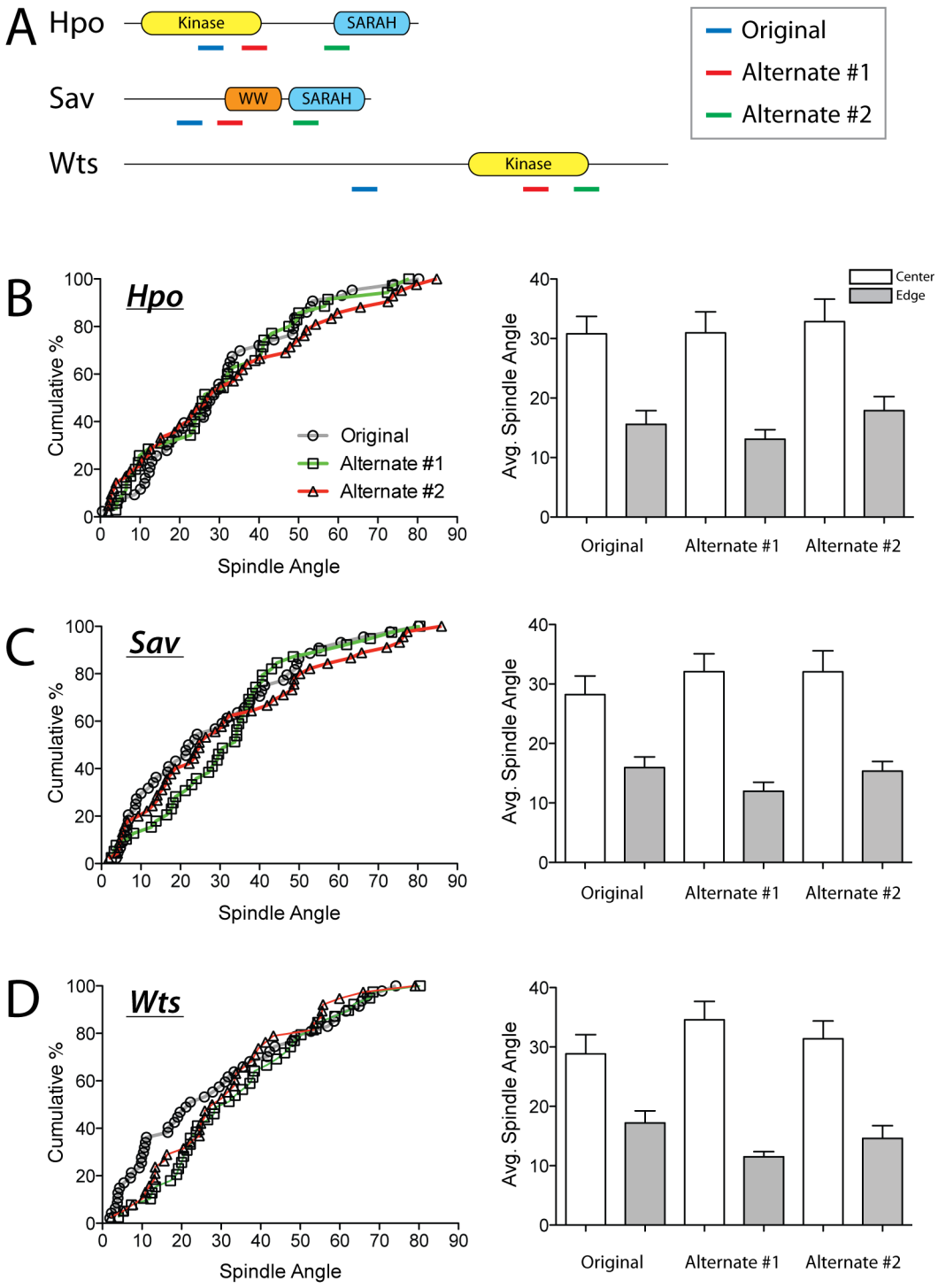

Figure S1, Related to Figure 2. RNAi targeted to alternative coding sequences within Hpo, Sav, and Wts cause spindle orientation defects in S2 cells.

(A) Domain architectures of Hippo (Hpo), Salvador (Sav), and Warts (Wts) proteins are shown with sites of RNAi targeted sequences depicted with blue, red, and green bars. Both alternative RNAi targets produce similar spindle orientation phenotypes for Hpo **(A)**, Sav **(B)**, and Wts **(C)**. In each case, the left panel shows cumulative percentage plots, whereas right panels show average spindle angles to an Ed:Pins crescent center (open bars) and edge (grey bars).

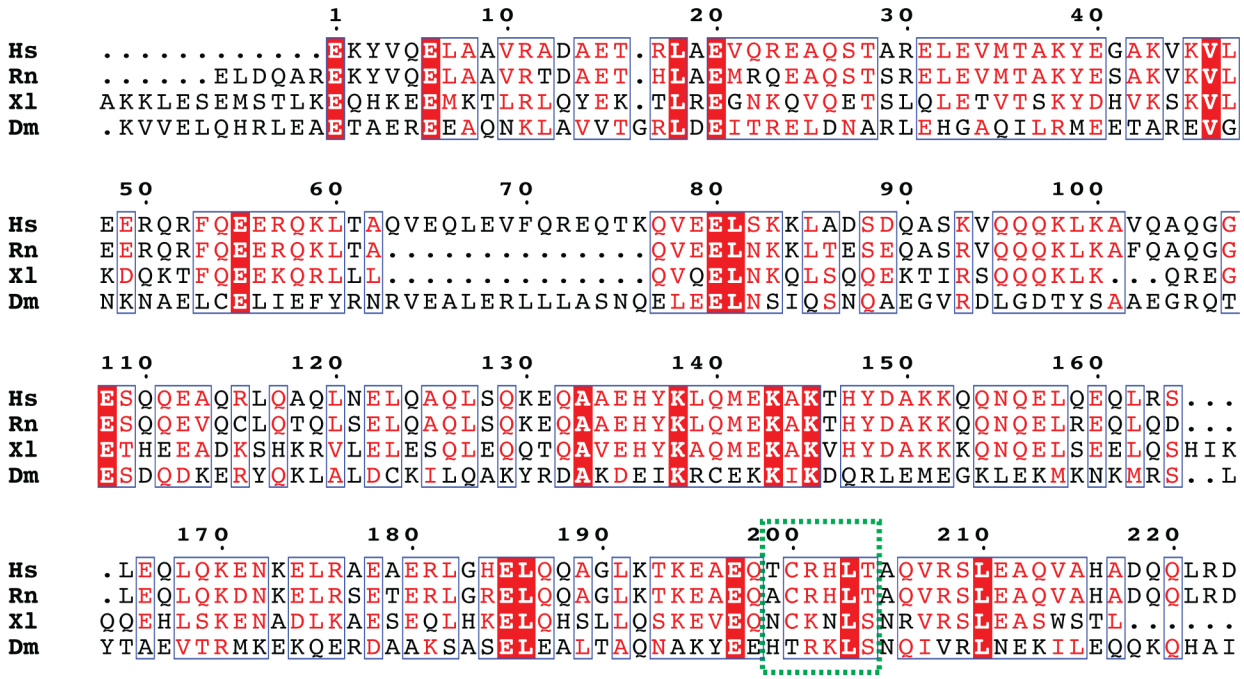

Figure S2, Related to Figure 4. Multiple sequence alignment of Mud^{CC} domains reveals conservation of Warts phosphorylation motif.

Alignment of multiple Mud^{CC} orthologous sequences (Hs: Human; Rn: Rat; Xl: Xenopus; Dm: Drosophila). Green dashed box indicates the local alignment of the Warts phosphorylation

motif. In addition to the phosphorylated S/T, each sequence contains a basic R/K residue at the -3 position. The preferred histidine at -5 is seen only in the fly sequence.

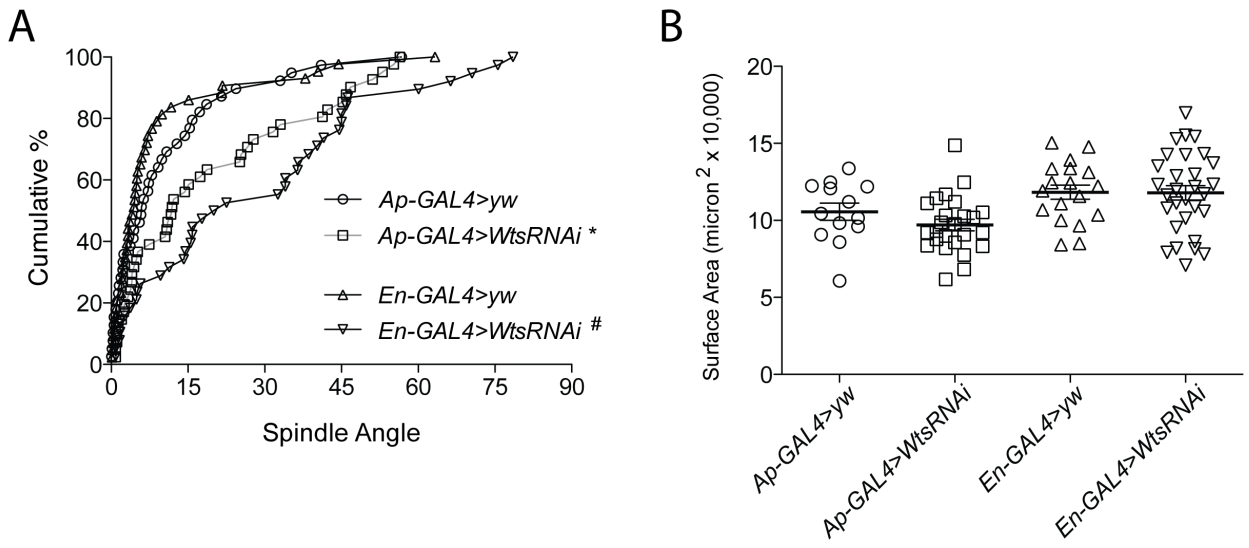

Figure S3, Related to Figure 7. Examination of wing disc phenotypes using alternative wing disc expressing GAL4 lines.

(A) Expression of Wts^{RNAi} using *Apterous-GAL4* (*Ap-GAL4)* or *Engrailed-GAL4* (*En-GAL4*) alternative wing disc drivers induces spindle orientation defects. *, $p < 0.05$ compared to respective control cross with yellow-white (yw) flies, ANOVA with Tukey's *post-hoc* test. **(B)** Wts^{RNAi} expression using *Ap-GAL4* or *En-GAL4* does not induce significant disc overgrowth. These results are both in general agreement with those presented for *Nub-GAL4* crosses in the main text.

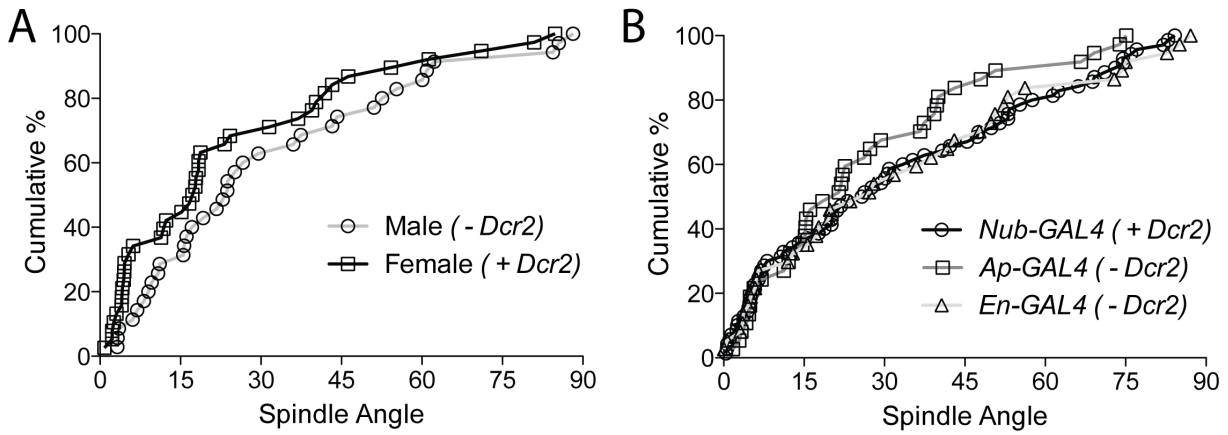

Figure S4, Related to Figure 7. Presence of Dicer2 (UAS-Dcr2) does not improve effectiveness of Mud^{RNAi} in inducing spindle orientation defects.

(A) Male *Nub-GAL4* flies (containing one UAS-Dcr2 on their X chromosome) were crossed with female Mud^{RNAi} flies (containing two wild-type X chromosomes). Male progeny of this cross thus lack UAS-Dcr2 (open circles), whereas female progeny have a single UAS-Dcr2 copy on an X chromosome (open squares). Spindle orientation did not differ between sexes indicating Mud^{RNAi} functions completely without the aid of Dcr2, consistent with its shRNA nature. **(B)** Expression of UAS-Mud^{RNAi} was achieved by crossing to *Ap-GAL4* (open squares) or *En-GAL4* (open triangles), which lack co-expression of UAS-Dcr2. Spindle orientation defects in these animals were similar to each other and did not differ significantly from those induced by *Nubbin-GAL4 (Nub-GAL4*, open circles), which does express one copy of UAS-Dcr2.

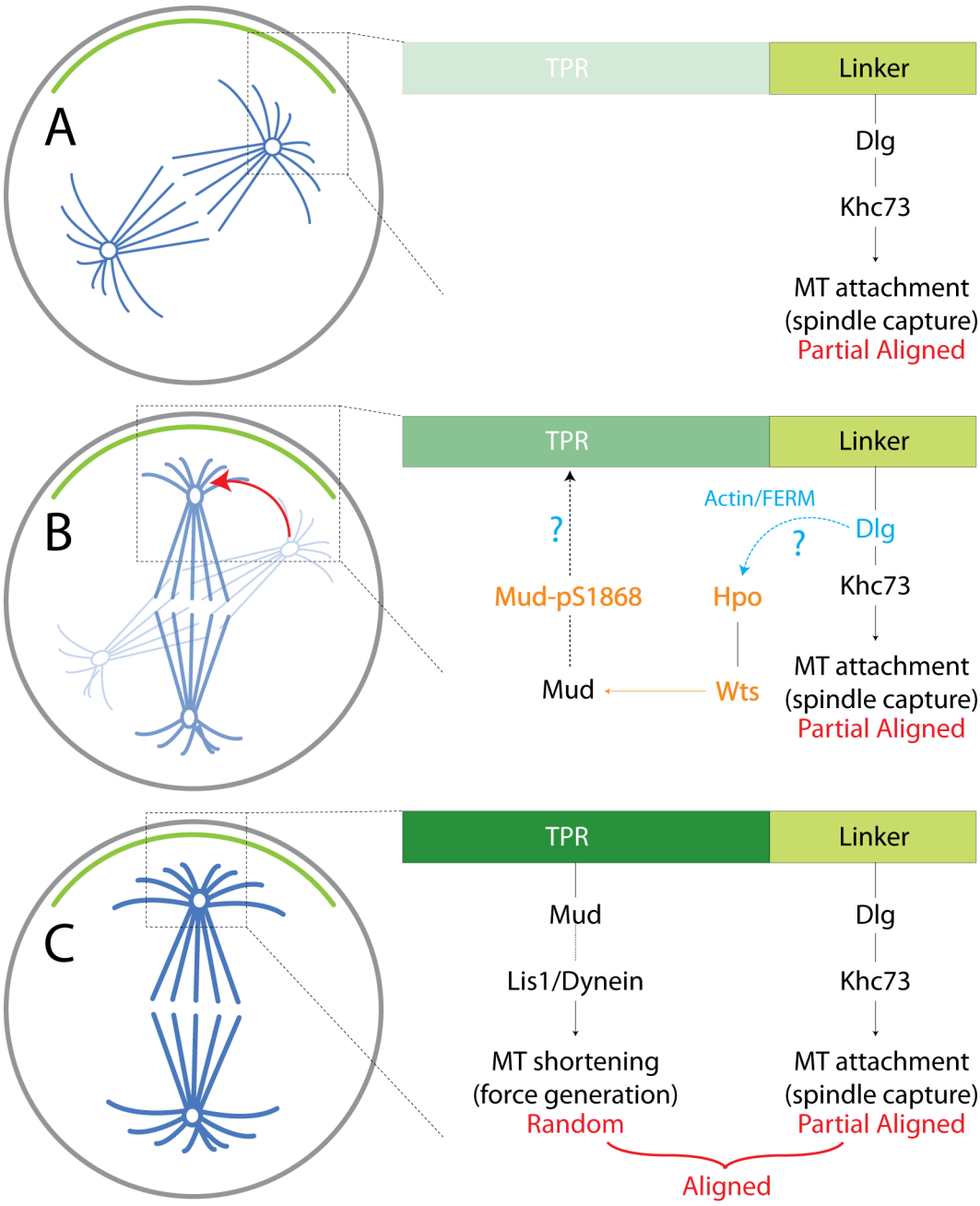

Figure S5. Proposed model for Warts-mediated regulation of the Pins/Mud spindle orientation pathway.

(A) Pins^{LINKER} initiates spindle orientation through Dlg/Khc73-mediated cortical capture of dynamic astral microtubules. This microtubule attachment provides a partially aligned spindle, which manifests as alignment to the edge of cortical cues seen in S2 cells (*see Figure 2*). **(B)** Engagement of the Mud-dependent pathway requires Mud to localize at the cell cortex with

Pins^{TPRs}. Results presented herein demonstrate that the core Hippo/Salvador/Warts complex is required for this process: phosphorylation of Mud by Warts promotes its cortical localization and activation of the Pins/Mud pathway. The upstream signals that activate this function of Hippo signaling remain to be identified, although the actin cytoskeleton and other polarity complexes are attractive candidates. Whether phosphorylation regulates additional Mud protein-protein interactions necessary for cortical recruitment also remains to be explored. **(C)** Upon Pins/Mud association, dynein-mediated spindle forces are activated, resulting in robust spindle alignment.